Loss of *Cnot6l* impairs inosine RNA modifications in mouse oocytes

Pavla Brachova [1]†ϕ, Nehemiah S. Alvarez [1]†, Lane K. Christenson [1]ϕ

[1] Department of Molecular and Integrative Physiology, University of Kansas Medical Center, Kansas City, KS 66160

† These authors contributed equally to this work

ϕ Corresponding Authors:

Pavla Brachova, PhD

3071 HLSIC

3901 Rainbow Blvd.

Kansas City, KS 66160

Phone: (913) 588-0421

E-mail: pbrachova@kumc.edu

Lane K. Christenson, PhD

3075 HLSIC

3901 Rainbow Blvd.

Kansas City, KS 66160

Phone: (913) 588-0420

Fax: (913) 588-7430

E-mail: lchristenson@kumc.edu

Author e-mail addresses: PB: pbrachova@kumc.edu; NSA: nalvarez@kumc.edu; LKC: lchristenson@kumc.edu

Abstract

Mammalian oocytes must degrade maternal transcripts through a process called translational mRNA decay, in which maternal mRNA undergoes translational activation, followed by deadenylation and mRNA decay. Once a transcript is translationally activated, it becomes deadenylated by the CCR4-NOT complex. Knockout of *Cnot6l*, a deadenylase within the CCR4-NOT complex, results in mRNA decay defects during MI entry. Knockout of *Btg4*, an adaptor protein of the CCR4-NOT complex, results in mRNA decay defects following fertilization. Therefore, mechanisms controlling mRNA turnover have significant impacts on oocyte competence and early embryonic development. Post-transcriptional inosine RNA modifications can impact mRNA stability, possibly through a translation mechanism. Here, we assessed inosine RNA modifications in oocytes from *Cnot6l*$^{-/-}$ and *Btg4*$^{-/-}$ mice, which display stabilization of mRNA and over-translation of the stabilized transcripts. If inosine modifications have a role in modulating RNA stability, we hypothesize that in these mutant backgrounds, we would observe changes or a disruption in inosine mRNA modifications. To test this, we used a computational approach to identify inosine RNA modifications in total and ribosome-associated mRNA-seq data during meiotic maturation (GV, MI, and MII stages). We observed pronounced depletion of inosine mRNA modifications in oocytes from *Cnot6l*$^{-/-}$, but not in *Btg4*$^{-/-}$ mice. Additionally, analysis of ribosome-associated RNA revealed clearance of inosine modified mRNA. These observations suggest a novel mechanism of mRNA clearance during oocyte maturation, in which inosine-containing transcripts decay in an independent, but parallel mechanism to CCR4-NOT deadenylation.

Introduction

Growing mammalian oocytes transcribe and store transcripts that support meiotic maturation, fertilization, and early embryo development (Bachvarova and De Leon 1980; Bachvarova 1985; De La Fuente et al. 2004; De La Fuente and Eppig 2001). The transition of

49 maternal to zygotic control of development is termed the maternal to zygotic transition (MZT),
50 and occurs in the absence of transcription (Piko and Clegg 1982; De La Fuente and Eppig
51 2001). As oocytes resume meiosis, a large-scale, but selective wave of maternal transcripts is
52 targeted for translation and subsequent degradation (Su et al. 2007; Svoboda et al. 2015; Sha
53 et al. 2019) in a process called translational mRNA decay. By the 2-cell stage of mouse early
54 embryogenesis, approximately 90% of maternal RNA are degraded (Schellander et al. 2007).
55 The activation of translation requires specific 3′ UTR elements, such as polyadenylation signals
56 and cytoplasmic polyadenylation elements (Chen et al. 2011; Dai et al. 2019). Once transcripts
57 undergo translational activation following the lengthening of their poly(A) tails, they are subject
58 to decay by deadenylation (Ozturk and Uysal 2017). CCR4-NOT is the major, multi-subunit
59 deadenylase complex involved in poly(A) shortening (Collart and Panasenko 2012). A functional
60 CCR4-NOT complex is essential for the proper decay of maternal oocyte mRNA, and for the
61 development of a fertilized oocyte into an embryo (Sha et al. 2018; Horvat et al. 2018; Yu et al.
62 2016; Dumdie et al. 2018).

63 An understanding of the individual components of the CCR4-NOT complex has
64 illuminated specific features of mRNA transcripts leading to their specific and selective decay.
65 The ribonuclease *Cnot6l* is uniquely expressed in mouse oocytes, and regulates deadenylation
66 of transcripts undergoing translational mRNA decay during oocyte maturation (Sha et al. 2018;
67 Horvat et al. 2018; Vieux and Clarke 2018). *Cnot6l*$^{-/-}$ mice are severely subfertile due to the
68 overtranslation of undegraded maternal transcripts, resulting in spindle defects during the
69 completion of meiosis (Sha et al. 2018; Horvat et al. 2018). The CCR4-NOT deadenylase
70 complex also relies on the adaptor RNA binding proteins, ZFP36L2 and BTG4, to associate with
71 cytoplasmic transcripts (Ball et al. 2014; Dumdie et al. 2018; Doidge et al. 2012; Liu et al. 2016;
72 Wu and Dean 2016; Pasternak et al. 2016). Z*fp36l2*$^{-/-}$ mice are infertile due to decreased oocyte
73 numbers as well as decreased rates of oocyte maturation (Ball et al. 2014; Dumdie et al. 2018).

74 *Btg4*$^{-/-}$ mice are also infertile due to embryonic arrest at the 2-cell and 4-cell stages (Yu et al.
75 2016; Sha et al. 2018). Cumulatively, these models demonstrate that the translational mRNA
76 decay machinery is necessary to establish the correct dosage of RNA during the MZT, and
77 dysfunction or loss of critical components within the mRNA degradation pathway leads to
78 infertility.

79 Previous work has established inosine post-transcriptional RNA modifications can impact mRNA
80 stability through a translation mechanism (Licht et al. 2019). Since the *Cnot6l*$^{-/-}$ and *Btg4*$^{-/-}$ mice
81 result in stabilization of mRNA and overtranslation of stabilized transcripts, we hypothesized that
82 in these mutant backgrounds, we would observe an increase in inosine modifications in mRNA.
83 Surprisingly, we observed a significant decrease in inosine modifications in oocytes from *Cnot6l*$^{-}$
84 $^{/-}$, but not in *Btg4*$^{-/-}$ mice, suggesting that in the absence of *Cnot6l*, mRNA degradation of
85 inosine-modified transcripts is still occurring, while unmodified transcripts are stabilized. Our
86 data suggest novel components of translational mRNA decay during oocyte maturation.

87 **Results**

88 *Inosine RNA modifications are lost in oocytes from Cnot6l*$^{-/-}$ mice

89 Using our computational approach (Brachova et al. 2019), we identified transcriptome wide
90 inosine RNA modifications (Supplemental Fig. S1) in previously reported RNA-seq datasets
91 (Sha et al. 2018) from wild-type (WT), *Cnot6l*$^{-/-}$, *Btg4*$^{-/-}$ oocytes at 0, 8, and 16 h after in vitro
92 maturation. These three time points correspond to the GV, MI, and MII oocyte stages,
93 respectively. The number of unique transcripts with inosine RNA modifications in *Cnot6l*$^{-/-}$
94 oocytes (134 ± 28 in GV, 159 ± 0 in MI, 163 ± 3 in MII, and 160 ± 7 in Zyg; Mean ± SEM) were
95 significantly lower than both WT oocytes and *Btg4*$^{-/-}$ oocytes at all oocyte/embryo stages (WT:
96 1750 ± 337 in GV, 999 ± 109 in MI, 1132 ± 213 in MII, and 1311 ± 562 in Zyg; *Btg4*$^{-/-}$: 1749 ±
97 197 in GV, 1412 ± 30 in MI, 1579 ± 103 in MII, and 1441 ± 200 in Zyg; one-way ANOVA; Fig.
98 1a). No difference in number of transcripts with inosine RNA modifications was detected

99 between WT and *Btg4*$^{-/-}$ oocytes at any stage (Fig. 1a). To confirm that the reduction in
100 transcripts with inosine RNA modifications in *Cnot6l*$^{-/-}$oocytes was not due to a differential
101 pattern of RNA expression, we identified inosine modifications only in transcripts found in all
102 samples across all groups (8,686 transcripts, total RNA; 6,006 transcripts, ribosome-associated
103 transcripts). The results (Fig. 1c), indicate that the loss of inosine RNA modification was not due
104 to differential gene expression.

105 *Inosine RNA modifications are enriched in ribosome-associated mRNA*

106 Our previous study linked inosine RNA modifications to the process of translation through RNA
107 modifications of codons (Brachova et al. 2019). To test if the accumulated and over-translated
108 maternal transcripts found in oocytes of *Cnot6l*$^{-/-}$ mice were enriched in inosine RNA
109 modifications, we cataloged inosine RNA modifications in ribosome-associated mRNA at the
110 GV, MI, and MII stages in WT and *Cnot6l*$^{-/-}$ oocytes. In the ribosome-associated mRNA of WT
111 GV oocytes, the number of inosine-modified transcripts decreased during oocyte maturation,
112 possibly indicating clearance of inosine-modified transcripts (Fig. 1b). Conversely, in *Cnot6l*$^{-/-}$
113 oocytes, significantly fewer transcripts are inosine-modified at the GV stage, and the number of
114 inosine-modified transcripts increases, rather than decreases during oocyte maturation (Fig.
115 1b). Even among commonly expressed transcripts, the pattern is similar (Fig. 1d). Our data
116 show that globally, the total RNA fraction of *Cnot6l*$^{-/-}$ oocytes have fewer inosine modified
117 transcripts, however, these modified transcripts are still detected in the ribosome-associated
118 fraction.

119 *Pattern of inosine RNA modifications in total and ribosome-associated mRNA*

120 In addition to having the fewest inosine modified transcripts, oocytes from *Cnot6l*$^{-/-}$ mice had the
121 lowest proportion of the transcriptome that was modified (GV: 1.0 ± 0.3%, MI: 1.2 ± 0.02%,
122 MII:1.2 ± 0.03%, Zyg: 1.3 ± 0.05%), compared to WT oocytes (GV: 14.4 ± 2.6%, MI: 8.5 ±
123 0.7%, MII: 10.1 ± 1.7%, Zyg: 10.9 ± 4.3%) and *Btg4*$^{-/-}$ oocytes (GV: 13.4 ± 1.2%, MI: 10.6 ±

124 0.3%, MII: 13.0 ± 0.7%, Zyg: 12.0 ± 1.4%; x^2 $p<0.5$; Fig. 2a). Among ribosome-associated
125 mRNA, a lower proportion of transcripts were modified in *Cnot6l*$^{-/-}$ oocytes (GV: 6.1 ± 0.2%, MI:
126 9.7 ± 0.2%, MII: 8.7 ± 0.4%,), compared to WT oocytes (GV: 16.4 ± 0.3%, MI: 10.6 ± 0.2%, MII:
127 9.5 ± 0.1%, Fig. 2b). Comparing the number of identified inosine RNA modifications per
128 transcript, on average, WT oocytes and *Btg4*$^{-/-}$ oocytes had similar patterns, while *Cnot6l*$^{-/-}$
129 oocytes contained transcripts with fewer modifications per transcript (blue and green lines, Fig.
130 2c). However, within ribosome-associated mRNA, the pattern of inosine RNA modifications per
131 transcript was similar (Fig. 2c). To further characterize the nature of inosine RNA modifications
132 in oocytes from WT, *Cnot6l*$^{-/-}$, and *Btg4*$^{-/-}$ mice, the location of modifications within protein-coding
133 genes was determined by annotating the location of each inosine RNA modification (5′ UTR,
134 coding, intron, and 3′ UTR). Overall, the distribution of inosine RNA modifications is similar
135 between all stages of oocyte maturation in WT and *Btg4*$^{-/-}$ mice, with the majority of
136 modifications occurring in the CDS and 3′ UTR. Conversely, oocytes from *Cnot6l*$^{-/-}$ mice display
137 a higher proportion of intron inosine RNA modifications (Fig. 2d). Within transcripts from
138 ribosome-associated mRNA, the pattern of inosine RNA modifications was similar (Fig. 2d).

139 *Consequences of coding sequence inosine RNA modifications in mouse oocytes*

140 To understand the consequence of inosine RNA modifications, if any, on the protein coding
141 capacity of mRNA transcripts, we used Ensembl Variant Effect Predictor (VEP) (McLaren et al.
142 2016) to identify the synonymous and non-synonymous substitutions (Fig. 3a). Among the non-
143 synonymous substitutions, altered stop codons (stop loss, stop gain, or stop retained) made up
144 less than 0.3% of coding sequence modifications. Therefore, stop codon substitutions were not
145 included in further analyses.

146 The majority of coding region inosine RNA modifications observed resulted in synonymous
147 substitutions in WT and *Btg4*$^{-/-}$ oocytes (Brachova et al. 2019) Conversely, in oocytes from
148 *Cnot6l*$^{-/-}$ oocytes, the pattern of inosine RNA modifications was reversed, with more than 60%

149 exhibiting non-synonymous substitutions (Fig. 3a). Inosine RNA modified transcripts in the
150 ribosome-associated mRNA had a similar pattern between WT and *Cnot6l*$^{-/-}$ oocytes (Fig. 3b). In
151 order to predict the consequence of the amino acid substitutions, a computational tool, Sorting
152 Intolerant From Tolerant (SIFT) that predicts the effects of amino acid substitution on protein
153 function was used (Ng and Henikoff 2003). SIFT analysis showed that inosine RNA
154 modifications observed in WT and *Btg4*$^{-/-}$ oocytes exhibited greater levels of tolerated amino
155 acid substitutions when compared to the oocytes from *Cnot6l*$^{-/-}$ mice (Fig. 3c). Again, inosine
156 RNA modified transcripts in the ribosome-associated mRNA had a similar pattern of tolerated
157 amino acid substitutions between WT and *Cnot6l*$^{-/-}$ oocytes (Fig. 3d). When considering the
158 number of tolerated or deleterious substitutions, *Cnot6l*$^{-/-}$ oocytes have reduced numbers in total
159 RNA (Fig. 3e), but in the ribosome-associated transcripts, only GV *Cnot6l*$^{-/-}$ oocytes had
160 significantly fewer tolerated substitutions (2-way ANOVA, $p < 0.05$, Fig. 3f). In summary, the
161 total RNA fraction in *Cnot6l*$^{-/-}$ oocytes had a higher proportion of inosine RNA modifications
162 within the coding sequencing that resulted in potentially deleterious non-synonymous
163 substitutions. However, within the ribosome-associated RNA, similar levels of synonymous and
164 non-synonymous and tolerated and deleterious substitutions were observed between WT and
165 *Cnot6l*$^{-/-}$. These results suggest that translated mRNA in WT and *Cnot6l*$^{-/-}$ oocytes share a
166 similar capacity for inosine induced protein recoding through alterations to codon usage.

167 *Inosine RNA modifications are enriched at the wobble position in ribosome-associated RNA*

168 The abundance of inosine modifications resulting in synonymous substitutions in WT and *Btg4*$^{-/-}$
169 oocyte RNA led us to investigate the potential effects of inosine RNA modifications on codon
170 usage. We first determined the number of inosine RNA modifications that occur in the 34
171 different codons that contain an adenosine, excluding stop codons. We found in WT and *Btg4*$^{-/-}$
172 oocytes, certain codons contain more inosine RNA modifications: AAA, ACA, CAA, CCA, GAA,
173 and GCA (Fig. 4a). In *Cnot6l*$^{-/-}$ oocytes, inosine-modified codons were significantly reduced

174 compared with WT and *Btg4*$^{-/-}$ oocytes (Fig. 4a). Additionally, there were no enriched modified
175 codons detected in *Cnot6l*$^{-/-}$ oocytes (Fig. 4a). Within transcripts from ribosome-associated
176 mRNA in both WT and *Cnot6l*$^{-/-}$ oocytes, we detected similar codons enriched in inosine RNA
177 modifications (Fig. 4b). Further analysis indicated that inosine modifications are enriched at the
178 wobble position in codons with multiple adenosines in total RNA of WT (Fig. 4c), but not in
179 *Cnot6l*$^{-/-}$ oocytes. Conversely, both WT and *Cnot6l*$^{-/-}$ ribosome-associated mRNA exhibited the
180 wobble position enhancement (Fig. 4d). The wobble position RNA modification across all
181 codons was not present in *Cnot6l*$^{-/-}$ oocytes in total RNA, in contrast to WT and *Btg4*$^{-/-}$ oocytes,
182 while the ribosome-associated mRNA retained wobble position inosine RNA modifications
183 across all three genotypes (Fig. 4e and f). Other codons assessed did not show a specific
184 enrichment or difference between WT and *Cnot6l*$^{-/-}$ oocytes (Supplemental Fig. S2).

185 *Efficiency of inosine RNA modifications is highest in ribosome-associated mRNA*

186 Transcriptome-wide inosine RNA modification efficiency at various codons remained around
187 50% throughout oocyte maturation and in the zygote in WT oocytes (Fig. 5a, raw counts are in
188 Supplemental Fig. 3). Conversely, *Cnot6l*$^{-/-}$ oocytes displayed defects in inosine RNA
189 modification efficiency in total RNA at all stages of oocyte maturation and in zygotes (Fig. 5a).
190 An examination of inosine RNA modification efficiency in *Btg4*$^{-/-}$ oocytes revealed a reduction of
191 modification efficiency of select codons (Fig. 5a). The inosine RNA modification efficiency
192 reached almost 100% within transcripts of ribosome-associated mRNA of WT oocytes, and then
193 decreased during oocyte maturation (Fig. 5b). *Cnot6l*$^{-/-}$ oocytes also displayed almost 100%
194 efficiency of particular codons (AAA, AAC, AAT, AGA, CAA, CAG, CCA, CGA, GTA, TTA), however
195 other codons were not modified at all (AAG, ACG, ACT, AGG, ATT, GAC, GAG, GAT), as seen in
196 Fig. 4. By the end of oocyte maturation, the inosine RNA modification efficiency was completely
197 lost (Fig. 5b). Overall, during oocyte maturation, the inosine RNA modification efficiency is
198 almost 100% in ribosome-associated mRNA, and decreases during maturation. These results

199 suggest that, in the *Cnot6l*$^{-/-}$ oocytes where mRNA is stabilized, the inosine modified mRNA are
200 degraded, while the unmodified mRNA stabilized.

201 **Discussion**

202 Translational mRNA decay is a main mechanism of maternal mRNA clearance in mammalian
203 oocytes. During oocyte maturation, mRNA are recruited for translation and subsequent
204 degradation through interactions with components of the CCR4-NOT complex (Sha et al. 2018;
205 Vieux and Clarke 2018). The maternal-to-zygotic decay machinery component CNOT6L plays
206 an important role in maternal mRNA decay during MI (Sha et al. 2018; Vieux and Clarke 2018;
207 Horvat et al. 2018), while the adaptor factor BTG4 plays an important role in degradation of
208 maternal mRNA after ovulation and prior to fertilization (Liu et al. 2016; Yu et al. 2016). As such,
209 selective decay of transcripts allows for specific control of events occurring during the MZT,
210 necessary for early embryo development.

211 An important component of translational mRNA decay is the rate of translation, which is
212 influenced by codon composition, a phenomenon known as codon optimality (Presnyak et al.
213 2015; Bazzini et al. 2016; Carneiro et al. 2019; Horstick et al. 2015; Pop et al. 2014; Bergman
214 and Tuller 2020). Codons that are non-optimal slow the ribosome, and experimental evidence
215 indicates that this increases mRNA degradation through CCR4-NOT (Webster et al. 2018). It
216 has recently been reported that inosine RNA modifications in the coding sequence of mRNA
217 lead to ribosome stalling (Licht et al. 2019). In a previous report (Brachova et al. 2019), and now
218 here in WT and *Btg4*$^{-/-}$ oocytes, we identified inosine RNA modifications specifically enriched in
219 at the codon wobble position in oocytes (Brachova et al. 2019). Based on our finding and
220 others, we hypothesized that inosine RNA modifications within the coding sequence could alter
221 mRNA stability, potentially through translational mRNA decay. To test this hypothesis we
222 analyzed previously generated RNA-seq data for *Cnot6l*$^{-/-}$ and *Btg4*$^{-/-}$ oocytes, which are known
223 to exhibit dysfunction in translational mRNA decay (Sha et al. 2018). The nearly complete loss

224 of inosine RNA modified transcripts in the *Cnot6l*$^{-/-}$ oocytes was unexpected, as we originally
225 hypothesized to identify increased modified transcripts in oocytes with hyper-stabilized mRNA
226 as previously established (Sha et al. 2018). The loss of inosine RNA modifications was not
227 associated with a loss of *Adar* expression (Supplemental Fig. S4), but we have not evaluated
228 ADAR protein levels in *Cnot6l*$^{-/-}$ oocytes, which is an important consideration. *Btg4*$^{-/-}$ oocytes, on
229 the other hand, have inosine RNA modification profiles similar to that of WT oocytes. Both
230 CNOT6L and BTG4 accumulate during oocyte maturation and trigger maternal mRNA decay,
231 but their knockouts result in different oocyte phenotypes: *Cnot6l*$^{-/-}$ oocytes arrest at
232 prometaphase I, while *Btg4*$^{-/-}$ oocytes are able to complete meiotic maturation and do not arrest
233 until fertilization (Sha et al. 2018). CNOT6L and BTG4 degradation pathways act on similar
234 substrate pools during oocyte maturation, albeit with different timing (Sha et al. 2018). We
235 identified inosine modified transcripts common between all genotypes, and observed that
236 *Cnot6l*$^{-/-}$ oocytes had significantly fewer modified transcripts compared to WT and *Btg4*$^{-/-}$
237 oocytes (Fig. 1c). We consider three possible mechanisms that can explain our results. First,
238 CONT6L and ADAR could interact in oocytes, facilitating inosine RNA modifications. Biological
239 evidence for such a complex is lacking. Recent mass spectrometry approaches to identify
240 ADAR associated proteins that regulate inosine RNA modifications have not identified CCR4-
241 NOT complex components (Freund et al. 2020). Rather, several components of the ribosome
242 were identified directly associated with ADAR (Freund et al. 2020).

243 The second explanation for reduced inosine RNA modifications in *Cnot6l*$^{-/-}$ oocytes is that *Adar*
244 is no longer being translated efficiently and the ADAR protein level is reduced, thus reducing
245 inosine RNA modifications. Though RNA abundance is not direct evidence for translation, we
246 detected *Adar* transcripts in *Cnot6l*$^{-/-}$ oocytes in both the total RNA and ribosome-associated
247 fractions (Supplemental Fig. S4). Additionally, it has been reported that *Cnot6l*$^{-/-}$ oocytes over-
248 translate mRNA (Sha et al. 2018). Based on these observations, we would anticipate that *Adar*

249 would have a higher probability to be over-translated rather than under-translated. Furthermore,
250 analysis of the ribosome-associated mRNA revealed that the number of inosine modified
251 transcripts were similar between MI and MII stages in WT and *Cnot6l*$^{-/-}$ oocytes (Fig. 1b, d). This
252 indicates that within the ribosome-associated fraction, ADAR had similar levels of activity in WT
253 and *Cnot6l*$^{-/-}$ oocytes. We observed a significant difference in inosine modified mRNA between
254 WT and *Cnot6l*$^{-/-}$ GV oocytes (Fig. 1b, d), indicating the reduction of inosine RNA modifications
255 occurs prior to GV entry. Additionally, analysis of the number of inosine modifications per
256 transcript, codon wobble position modifications, and efficiency of modifications within ribosome-
257 associated mRNA revealed that both WT and *Cnot6l*$^{-/-}$ oocytes had similar levels of inosine RNA
258 modifications at the GV stage (Fig. 3c, 4f, & 5b). We have previously shown that the inosine
259 modification efficiency in oocytes is linked to the catalytic activity of ADAR (Brachova et al.
260 2019), indicating that ADAR is present and active in *Cnot6l*$^{-/-}$ oocytes. Therefore, we do not
261 consider a reduction of ADAR protein to be a likely explanation for the decrease in inosine RNA
262 modifications present in *Cnot6l*$^{-/-}$ oocytes, however, further experimentation would be needed to
263 test ADAR levels in the absence of CNOT6L.

264 A third possible mechanism to explain the reduction in inosine RNA modifications in *Cnot6l*$^{-/-}$
265 oocytes is that CONT6L and ADAR both contribute to translational mRNA degradation, through
266 two independent, but parallel pathways. An important component of translational mRNA decay
267 is the rate of translation, which is influenced by codon composition, a phenomenon known as
268 codon optimality (Presnyak et al. 2015; Bazzini et al. 2016; Carneiro et al. 2019). Codons that
269 are non-optimal slow the ribosome, and experimental evidence indicates that this increases
270 mRNA degradation through CCR4-NOT (Webster et al. 2018; Buschauer et al. 2020). It has
271 been reported that inosine RNA modifications in the coding sequence of mRNA lead to
272 ribosome stalling (Licht et al. 2019). In our previous report, we identified inosine RNA
273 modifications in the total RNA fraction that are specifically enriched at the codon wobble position

274 (Brachova et al. 2019). Here, we show that ribosome-associated mRNA have similar inosine
275 enrichment to the wobble position of codons in both WT and *Cnot6l*$^{-/-}$ oocytes (Fig. 4f).
276 However, codon wobble position enrichment of inosine is absent in the total RNA fraction
277 *Cnot6l*$^{-/-}$ oocytes (Fig. 4e). Furthermore, the number of transcripts with inosine RNA
278 modifications is significantly reduced in the total RNA fraction of *Cnot6l*$^{-/-}$ oocytes when
279 compared to WT (Fig. 1a). We reason that one explanation for the difference between the
280 amount of RNA transcripts with inosine RNA modifications between total RNA and ribosome-
281 associated mRNA fractions is due to the number of oocytes used and the subsequent
282 enrichment of ribosome fraction (total RNA: 10 oocytes; ribosome-associated RNA: 500
283 oocytes). The inosine modified transcripts in the ribosome fraction are also present in the total
284 RNA, albeit at a smaller proportion, and enrichment allows for their detection.

285 Additionally, the observed reduction of inosine RNA modifications in *Cnot6l*$^{-/-}$ oocytes within the
286 total RNA fraction may be due to two factors: overall increased mRNA stability and selective
287 decay of inosine modified mRNA. In *Cnot6l*$^{-/-}$ oocytes, mRNA is globally stabilized, and we
288 hypothesize that inosine modified RNA is targeted for decay. We reason that the stabilization of
289 mRNA increases the mRNA complexity of the total RNA fraction, thus reducing the sensitivity of
290 RNA-seq to detect inosine modified RNAs. The same phenomenon is present in the ribosome-
291 associated fraction of *Cnot6l*$^{-/-}$ oocytes, but it is offset by the enrichment procedure of ribosome.
292 In the ribosome-associated fraction, we were able to observe that in the GV oocyte stage of WT
293 and *Cnot6l*$^{-/-}$ oocytes, inosine RNA modification efficiency was above 60%, and in some cases
294 almost 100% for the codons analyzed (Fig. 5b). In comparison, the total RNA fraction, inosine
295 modification efficiency was approximately 50% (Fig. 5a). In the ribosome-associated fraction of
296 WT oocytes, progression into MI phase was marked by a reduction in inosine RNA modification
297 efficiency (Fig. 5b). In *Cnot6l*$^{-/-}$ oocytes, there is almost a complete loss of inosine RNA
298 modification efficiency at the codons analyzed (Fig. 5b). An interpretation of this observation is

299 that inosine mRNA are subject to a decay process independent of CNOT6L. In ribosome-
300 associated mRNA of WT oocytes, we observe a reduction of inosine containing mRNA, and this
301 reduction is similar to the reduction in overall mRNA levels at MI (Sha et al. 2018). We
302 hypothesize that mRNA decay mediated by CNOT6L and inosine RNA modifications share a
303 common component: translation. It has previously been shown that inosine RNA modifications
304 in coding sequences can induce ribosome stalling (Licht et al. 2019). Stalling, or slowing of
305 ribosomes can induce CCR4-NOT decay (Webster et al. 2018; Buschauer et al. 2020). Based
306 on this prediction, we had originally hypothesized that we would observe increases in inosine
307 RNA modifications in *Cnot6l*$^{-/-}$ oocytes. However, we observed a decrease in inosine RNA
308 modifications in the ribosomal associated fraction. If the inosine induced stalling or slowing of
309 ribosomes is still occurring and in the absence of a functioning CCR4-NOT complex decay was
310 still progressing, this would indicate a parallel pathway to mRNA decay. Our results suggest a
311 novel mechanism of mRNA clearance during oocyte maturation, in which inosine-containing
312 transcripts decay uncoupled from CCR4-NOT deadenylation. Further experiments will reveal the
313 impact of inosine RNA modifications on maternal mRNA decay.

314 **Methods**

315 *Sources of GV and MII RNA-seq datasets*

316 Wild-type GV, MI, MII, and Zyote RNA-seq data, and GV, MI, MII, and Zygote RNA-seq data
317 from *Cnot6l*$^{-/-}$ and *Btg4*$^{-/-}$ knockout mice dataset PRJNA486094 (Sha et al. 2018). The authors of
318 this study generated library preparations from total RNA isolated from groups of 10 oocytes or
319 embryos, all on the C57B6 background. For RNA-seq libraries of polysome-bound mRNA,
320 groups of 500 oocytes or embryos were used for polysome pull-down. Two replicates were
321 generated for library preparation, and each preparation had mCherry spike-in added before
322 cDNA synthesis for normalization. Barcoded libraries were pooled and sequenced on an
323 Illumina HiSeq X Ten platform with 150 bp paired-end reads (Sha et al. 2018).

324 *Identification and consequence analysis of inosine RNA modifications*

325 We identified putative inosine RNA modifications utilizing a combination of the HISAT2 aligner,
326 the Genome Analysis Tool Kit (GATK), and Ensembl Variant Effect Predictor (VEP) (McKenna
327 et al. 2010; McLaren et al. 2016; Kim et al. 2015; Brachova et al. 2019). Inosines appear as A-
328 to-G substitutions when comparing RNA-seq data to a reference genome (Ramaswami et al.
329 2013). HISAT2 was used to map raw RNA-seq reads to a mus musculus index built from
330 GRCm38 containing common SNP annotation from dbSNP.

331 Default settings for HISAT2 were used for each type of library aligned (i.e. single-end, paired-
332 end, or stranded, Supplemental Table 2) (Kim et al. 2015). Prior to alignment, fastq files were
333 checked for adaptors and trimmed if necessary, using Trimmomatic (Bolger et al. 2014). The
334 default alignment settings for HISAT2 will report at most 10 valid primary alignments; we did not
335 increase the amount of multimapping allowed. HISAT2 reports valid alignments that are at or
336 above the minimum alignment score determined by the function where the length of the read.
337 Mismatches in the alignment were subtracted from the alignment score, reads that fell below the
338 minimum alignment score were not reported. RNA/DNA differences were called using the
339 Genome Analysis Toolkit (GATK) RNASeq variant pipeline with modifications (McKenna et al.
340 2010). The program elprep was used to sort, mark duplicates, and index RNA-seq reads.
341 Known SNPs were filtered out using the Mouse Genomes Project database, Wellcome Trust
342 Sanger Institute mouse strains (Yalcin et al. 2011). RNA-DNA mismatches identified by HISAT2,
343 regardless if stranded mode was used, and GATK were reported in the sense orientation;
344 therefore strand information of the variant is inferred from the gene model using Ensembl VEP
345 (McLaren et al. 2016). VCF files were filtered on allelic depth (AD > 0) and used as input for
346 Ensembl Variant Effect Predictor (VEP, (McLaren et al. 2016)). VEP was used to identify inosine
347 modified transcripts, categorize the location within the transcript; and determine the
348 consequence of inosines on coding capacity. Only inosine sites occurring in transcripts with

349 TPM ≥ 1 and having an AD > 0 were reported. A transcript was considered to be inosine

350 modified if it contained at least one inosine site. R statistical computation software with the

351 following packages was used to parse VEP output: sleuth, biomaRt, dplyr, plyr,

352 AnnotationFuncs, org.Mm.eg.db, ggplot2 (Pimentel et al. 2017; Team and Others 2013;

353 Wickham 2009; Durinck et al. 2009).

354 **References**

355 Bachvarova R. 1985. Gene expression during oogenesis and oocyte development in mammals.
356 *Dev Biol* **1**: 453–524.

357 Bachvarova R, De Leon V. 1980. Polyadenylated RNA of mouse ova and loss of maternal RNA
358 in early development. *Dev Biol* **74**: 1–8.

359 Ball CB, Rodriguez KF, Stumpo DJ, Ribeiro-Neto F, Korach KS, Blackshear PJ, Birnbaumer L,
360 Ramos SBV. 2014. The RNA-binding protein, ZFP36L2, influences ovulation and oocyte
361 maturation. *PLoS One* **9**: e97324.

362 Bazzini AA, Del Viso F, Moreno-Mateos MA, Johnstone TG, Vejnar CE, Qin Y, Yao J, Khokha
363 MK, Giraldez AJ. 2016. Codon identity regulates mRNA stability and translation efficiency
364 during the maternal-to-zygotic transition. *EMBO J* **35**: 2087–2103.

365 Bergman S, Tuller T. 2020. Widespread non-modular overlapping codes in the coding regions.
366 *Phys Biol*. http://dx.doi.org/10.1088/1478-3975/ab7083.

367 Bolger AM, Lohse M, Usadel B. 2014. Trimmomatic: a flexible trimmer for Illumina sequence
368 data. *Bioinformatics* **30**: 2114–2120.

369 Brachova P, Alvarez NS, Hong X, Gunewardena S, Vincent KA, Latham KE, Christenson LK.
370 2019. Inosine RNA modifications are enriched at the codon wobble position in mouse
371 oocytes and eggs. *Biol Reprod*. http://dx.doi.org/10.1093/biolre/ioz130.

372 Buschauer R, Matsuo Y, Sugiyama T, Chen Y-H, Alhusaini N, Sweet T, Ikeuchi K, Cheng J,
373 Matsuki Y, Nobuta R, et al. 2020. The Ccr4-Not complex monitors the translating ribosome
374 for codon optimality. *Science* **368**. http://dx.doi.org/10.1126/science.aay6912.

375 Carneiro RL, Requião RD, Rossetto S, Domitrovic T, Palhano FL. 2019. Codon stabilization
376 coefficient as a metric to gain insights into mRNA stability and codon bias and their
377 relationships with translation. *Nucleic Acids Res* **47**: 2216–2228.

378 Chen J, Melton C, Suh N, Oh JS, Horner K, Xie F, Sette C, Blelloch R, Conti M. 2011. Genome-
379 wide analysis of translation reveals a critical role for deleted in azoospermia-like (Dazl) at
380 the oocyte-to-zygote transition. *Genes Dev* **25**: 755–766.

381 Collart MA, Panasenko OO. 2012. The Ccr4–Not complex. *Gene* **492**: 42–53.

382 Dai X-X, Jiang J-C, Sha Q-Q, Jiang Y, Ou X-H, Fan H-Y. 2019. A combinatorial code for mRNA
383 3′-UTR-mediated translational control in the mouse oocyte. *Nucleic Acids Research* **47**:
384 328–340. http://dx.doi.org/10.1093/nar/gky971.

385 De La Fuente R, Eppig JJ. 2001. Transcriptional activity of the mouse oocyte genome:
386 companion granulosa cells modulate transcription and chromatin remodeling. *Dev Biol* **229**:
387 224–236.

388 De La Fuente R, Viveiros MM, Burns KH, Adashi EY, Matzuk MM, Eppig JJ. 2004. Major
389 chromatin remodeling in the germinal vesicle (GV) of mammalian oocytes is dispensable for
390 global transcriptional silencing but required for centromeric heterochromatin function. *Dev*
391 *Biol* **275**: 447–458.

392 Doidge R, Mittal S, Aslam A, Winkler GS. 2012. The anti-proliferative activity of BTG/TOB
393 proteins is mediated via the Caf1a (CNOT7) and Caf1b (CNOT8) deadenylase subunits of
394 the Ccr4-not complex. *PLoS One* **7**: e51331.

395 Dumdie JN, Cho K, Ramaiah M, Skarbrevik D, Mora-Castilla S, Stumpo DJ, Lykke-Andersen J,
396 Laurent LC, Blackshear PJ, Wilkinson MF, et al. 2018. Chromatin Modification and Global
397 Transcriptional Silencing in the Oocyte Mediated by the mRNA Decay Activator ZFP36L2.
398 *Dev Cell* **44**: 392–402.e7.

399 Durinck S, Spellman PT, Birney E, Huber W. 2009. Mapping identifiers for the integration of
400 genomic datasets with the R/Bioconductor package biomaRt. *Nature Protocols* **4**: 1184–
401 1191. http://dx.doi.org/10.1038/nprot.2009.97.

402 Freund EC, Sapiro AL, Li Q, Linder S, Moresco JJ, Yates JR 3rd, Li JB. 2020. Unbiased
403 Identification of trans Regulators of ADAR and A-to-I RNA Editing. *Cell Rep* **31**: 107656.

404 Horstick EJ, Jordan DC, Bergeron SA, Tabor KM, Serpe M, Feldman B, Burgess HA. 2015.
405 Increased functional protein expression using nucleotide sequence features enriched in
406 highly expressed genes in zebrafish. *Nucleic Acids Res* **43**: e48.

407 Horvat F, Fulka H, Jankele R, Malik R, Jun M, Solcova K, Sedlacek R, Vlahovicek K, Schultz
408 RM, Svoboda P. 2018. Role of Cnot6l in maternal mRNA turnover. *Life Sci Alliance* **1**:
409 e201800084.

410 Kim D, Langmead B, Salzberg SL. 2015. HISAT: a fast spliced aligner with low memory
411 requirements. *Nat Methods* **12**: 357–360.

412 Licht K, Hartl M, Amman F, Anrather D, Janisiw MP, Jantsch MF. 2019. Inosine induces
413 context-dependent recoding and translational stalling. *Nucleic Acids Res* **47**: 3–14.

414 Liu Y, Lu X, Shi J, Yu X, Zhang X, Zhu K, Yi Z, Duan E, Li L. 2016. BTG4 is a key regulator for
415 maternal mRNA clearance during mouse early embryogenesis. *Journal of Molecular Cell*
416 *Biology* **8**: 366–368. http://dx.doi.org/10.1093/jmcb/mjw023.

417 McKenna A, Hanna M, Banks E, Sivachenko A, Cibulskis K, Kernytsky A, Garimella K, Altshuler
418 D, Gabriel S, Daly M, et al. 2010. The Genome Analysis Toolkit: a MapReduce framework
419 for analyzing next-generation DNA sequencing data. *Genome Res* **20**: 1297–1303.

420 McLaren W, Gil L, Hunt SE, Riat HS, Ritchie GRS, Thormann A, Flicek P, Cunningham F. 2016.

421 The Ensembl Variant Effect Predictor. *Genome Biol* **17**: 122.

422 Ng PC, Henikoff S. 2003. SIFT: Predicting amino acid changes that affect protein function.
423 *Nucleic Acids Res* **31**: 3812–3814.

424 Ozturk S, Uysal F. 2017. Poly(A)-binding proteins are required for translational regulation in
425 vertebrate oocytes and early embryos. *Reprod Fertil Dev* **29**: 1890–1901.

426 Pasternak M, Pfender S, Santhanam B, Schuh M. 2016. The BTG4 and CAF1 complex
427 prevents the spontaneous activation of eggs by deadenylating maternal mRNAs. *Open*
428 *Biology* **6**: 160184. http://dx.doi.org/10.1098/rsob.160184.

429 Piko L, Clegg KB. 1982. Quantitative changes in total RNA, total poly(A), and ribosomes in early
430 mouse embryos. *Dev Biol* **89**: 362–378.

431 Pimentel H, Bray NL, Puente S, Melsted P, Pachter L. 2017. Differential analysis of RNA-seq
432 incorporating quantification uncertainty. *Nat Methods* **14**: 687–690.

433 Pop C, Rouskin S, Ingolia NT, Han L, Phizicky EM, Weissman JS, Koller D. 2014. Causal
434 signals between codon bias, mRNA structure, and the efficiency of translation and
435 elongation. *Mol Syst Biol* **10**: 770.

436 Presnyak V, Alhusaini N, Chen Y-H, Martin S, Morris N, Kline N, Olson S, Weinberg D, Baker
437 KE, Graveley BR, et al. 2015. Codon optimality is a major determinant of mRNA stability.
438 *Cell* **160**: 1111–1124.

439 Ramaswami G, Zhang R, Piskol R, Keegan LP, Deng P, O'Connell MA, Li JB. 2013. Identifying
440 RNA editing sites using RNA sequencing data alone. *Nat Methods* **10**: 128–132.

441 Schellander K, Hoelker M, Tesfaye D. 2007. Selective degradation of transcripts in mammalian
442 oocytes and embryos. *Theriogenology* **68 Suppl 1**: S107–15.

443 Sha Q-Q, Yu J-L, Guo J-X, Dai X-X, Jiang J-C, Zhang Y-L, Yu C, Ji S-Y, Jiang Y, Zhang S-Y, et
444 al. 2018. CNOT6L couples the selective degradation of maternal transcripts to meiotic cell
445 cycle progression in mouse oocyte. *EMBO J*. http://dx.doi.org/10.15252/embj.201899333.

446 Sha Q-Q, Zhang J, Fan H-Y. 2019. A story of birth and death: mRNA translation and clearance
447 at the onset of Maternal-to-Zygotic transition in mammals. *Biol Reprod*.
448 http://dx.doi.org/10.1093/biolre/ioz012.

449 Su Y-Q, Sugiura K, Woo Y, Wigglesworth K, Kamdar S, Affourtit J, Eppig JJ. 2007. Selective
450 degradation of transcripts during meiotic maturation of mouse oocytes. *Dev Biol* **302**: 104–
451 117.

452 Svoboda P, Franke V, Schultz RM. 2015. Sculpting the Transcriptome During the Oocyte-to-
453 Embryo Transition in Mouse. *Curr Top Dev Biol* **113**: 305–349.

454 Team RC, Others. 2013. R: A language and environment for statistical computing.
455 http://cran.univ-paris1.fr/web/packages/dplR/vignettes/intro-dplR.pdf.

456 Vieux K-F, Clarke HJ. 2018. CNOT6 regulates a novel pattern of mRNA deadenylation during
457 oocyte meiotic maturation. *Sci Rep* **8**: 6812.

458 Webster MW, Chen Y-H, Stowell JAW, Alhusaini N, Sweet T, Graveley BR, Coller J, Passmore
459 LA. 2018. mRNA Deadenylation Is Coupled to Translation Rates by the Differential
460 Activities of Ccr4-Not Nucleases. *Mol Cell* **70**: 1089–1100.e8.

461 Wickham H. 2009. ggplot2: elegant graphics for data analysis.[WWW document]. *URL*
462 *https://cran r-project org/package= ggplot2 [accessed on 10 January 2016]*.

463 Wu D, Dean J. 2016. BTG4, a maternal mRNA cleaner. *J Mol Cell Biol* **8**: 369–370.

464 Yalcin B, Wong K, Agam A, Goodson M, Keane TM, Gan X, Nellåker C, Goodstadt L, Nicod J,
465 Bhomra A, et al. 2011. Sequence-based characterization of structural variation in the
466 mouse genome. *Nature* **477**: 326–329.

467 Yu C, Ji S-Y, Sha Q-Q, Dang Y, Zhou J-J, Zhang Y-L, Liu Y, Wang Z-W, Hu B, Sun Q-Y, et al.
468 2016. BTG4 is a meiotic cell cycle-coupled maternal-zygotic-transition licensing factor in
469 oocytes. *Nat Struct Mol Biol* **23**: 387–394.

470 **Figure Legends**

471 **Figure 1. Inosine RNA modifications occur in transcripts enriched in the ribosome-**

472 **associated RNA.** A-B) The number of unique inosine modified transcripts identified in WT,

473 *Cnot6l*$^{-/-}$, and *Btg4*$^{-/-}$ GV, MI, MII, and Zyg in total RNA (A) and ribosome-associated mRNA (B).

474 C-D) Among common transcripts present in all samples, the number of unique inosine modified

475 transcripts identified in WT, *Cnot6l*$^{-/-}$, and *Btg4*$^{-/-}$ GV, MI, MII, and Zyg in total RNA (C) and

476 ribosome-associated mRNA (D).

477 **Figure 2. Distinct pattern of inosine RNA modifications from WT, *Cnot6l*$^{-/-}$, and *Btg4*$^{-/-}$**

478 **oocytes and zygotes.** A-B) Proportion of the transcriptome (percentage) that contains inosine

479 RNA modifications in total RNA (A) and ribosome-associated mRNA (B). C) Number of inosine

480 RNA modified transcripts exhibiting one or multiple inosines per transcript in total RNA and

481 ribosome-associated RNA. Numbers above line indicate the number of inosines / transcript. D)

482 Number of inosine RNA modifications within specific regions (5′ UTR, CDS, intron, and 3′ UTR)

483 in mRNA in total RNA and ribosome-associated RNA. *Means ± SEM within panel A and B are

484 different ($p < 0.05$); significance was determined using 2 tests. Only transcripts with TPM ≥ 1

485 were analyzed.

486 **Figure 3. Consequences of inosine RNA modifications within CDS from WT, *Cnot6l*$^{-/-}$, and**
487 ***Btg4*$^{-/-}$ oocytes and zygote transcripts.** A-B) Proportion of inosine modifications (percentage)
488 in WT, *Cnot6l*$^{-/-}$, and *Btg4*$^{-/-}$ oocytes and zygotes that result in non-synonymous or synonymous
489 changes was determined for all CDS inosine modified mRNA transcripts in total RNA (A) and
490 ribosome-associated mRNA (B). C-D) Proportion of tolerated and deleterious transcripts
491 following Sorting Intolerant From Tolerant (SIFT) analysis of the inosine modified mRNA
492 transcripts from WT, *Cnot6l*$^{-/-}$, and *Btg4*$^{-/-}$ oocytes and zygotes in total RNA (C) or ribosome-
493 associated mRNA (D). E-F) Counts of tolerated and deleterious transcripts resulting from
494 inosine RNA modifications from WT, *Cnot6l*$^{-/-}$, and *Btg4*$^{-/-}$ oocytes and zygotes in total RNA (E)
495 or ribosome-associated mRNA (F). *Means ± SEM within a panel are different ($p < 0.05$);
496 significance was determined using X2 tests or 2-way ANOVA. Only transcripts with TPM ≥ 1
497 were analyzed.

498 **Figure 4. Inosines are enriched at the wobble position of codons in total RNA and**
499 **ribosome-associated RNA.** A-B) Number of inosine RNA modifications in adenosine-
500 containing codons in WT, *Cnot6l*$^{-/-}$, and *Btg4*$^{-/-}$ oocytes and zygotes in total RNA (A) and
501 ribosome-associated RNA (B). C-D) Number of inosine RNA modifications occurring at specific
502 codons among the codons with multiple adenosines in WT, *Cnot6l*$^{-/-}$, and *Btg4*$^{-/-}$ oocytes and
503 zygotes in total RNA (C) and ribosome-associated RNA (D). E-F) Global frequency of inosine
504 RNA modifications at the first, second, or third codon positions in WT, *Cnot6l*$^{-/-}$, and *Btg4*$^{-/-}$
505 oocytes and zygotes in total RNA (E) and ribosome-associated RNA (F). *Means ± SEM within
506 a panel were different ($p < 0.05$); significance was determined using two-way ANOVA tests.
507 Only codons from transcripts with TPM ≥ 1 were analyzed.

508 **Figure 5. Inosine RNA modification efficiency of total and ribosome-associated mRNA.** A)
509 Inosine RNA modification efficiency in total RNA from WT, *Cnot6l*$^{-/-}$, and *Btg4*$^{-/-}$ oocytes and

510 zygotes. Capital letter denotes the position of the codon with an inosine RNA modification. B)

511 Inosine RNA modification efficiency in ribosome-associated mRNA from WT and *Cnot6l*$^{-/-}$

512 oocytes and zygotes. Capital letter denotes the position of the codon with an inosine RNA

513 modification.

Figure 1

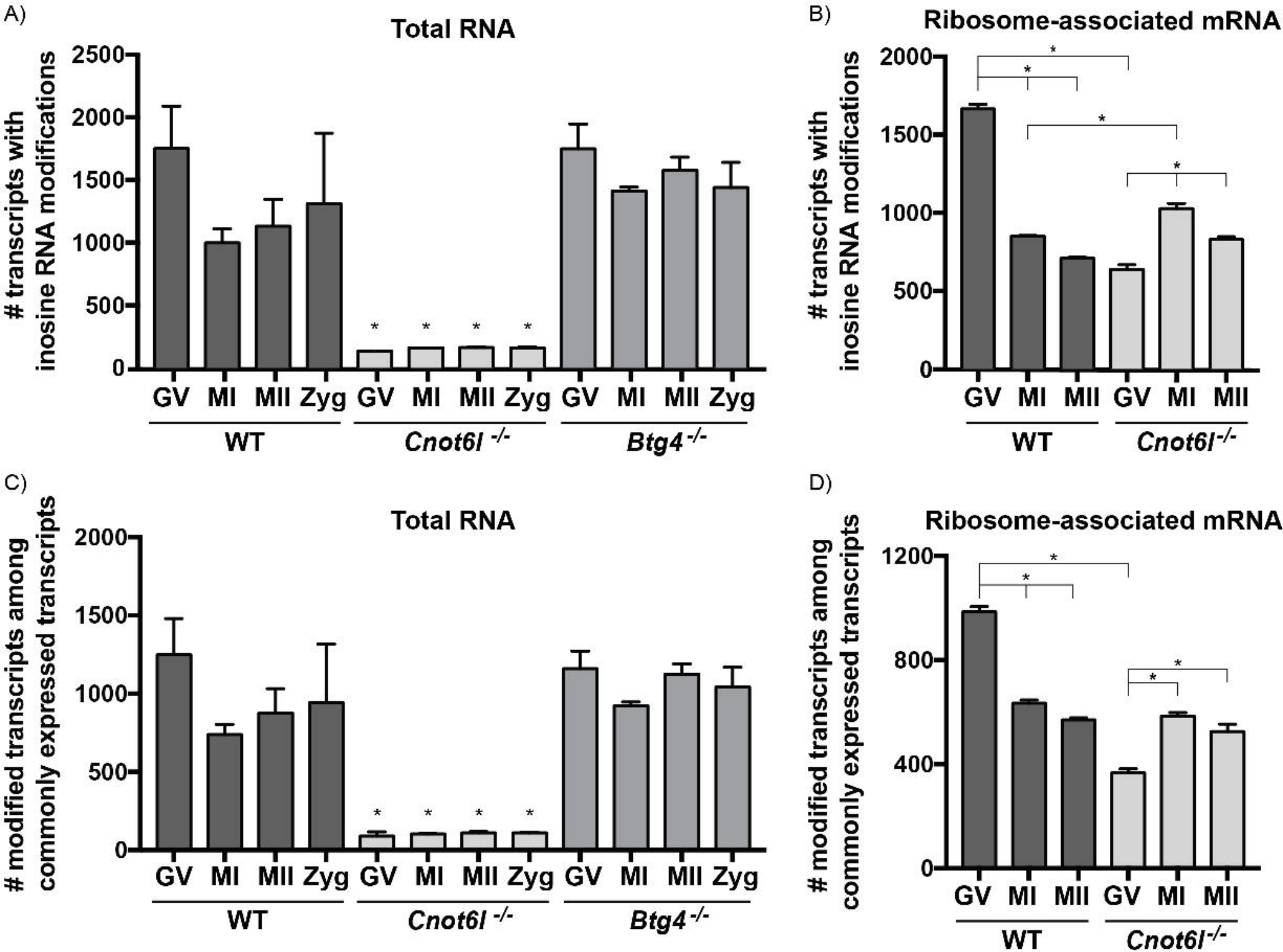
A)
Total RNA
transcripts with inosine RNA modifications
2500
2000
1500
1000
500
0
GV MI MII Zyg GV MI MII Zyg GV MI MII Zyg
WT
Cnot6l -/-
Btg4 -/-
B)
Ribosome-associated mRNA
transcripts with inosine RNA modifications
2000
1500
1000
500
0
GV MI MII GV MI MII
WT
Cnot6l -/-
C)
Total RNA
modified transcripts among commonly expressed transcripts
2000
1500
1000
500
0
GV MI MII Zyg GV MI MII Zyg GV MI MII Zyg
WT
Cnot6l -/-
Btg4 -/-
D)
Ribosome-associated mRNA
modified transcripts among commonly expressed transcripts
1200
800
400
0
GV MI MII GV MI MII
WT
Cnot6l -/-

Figure 2

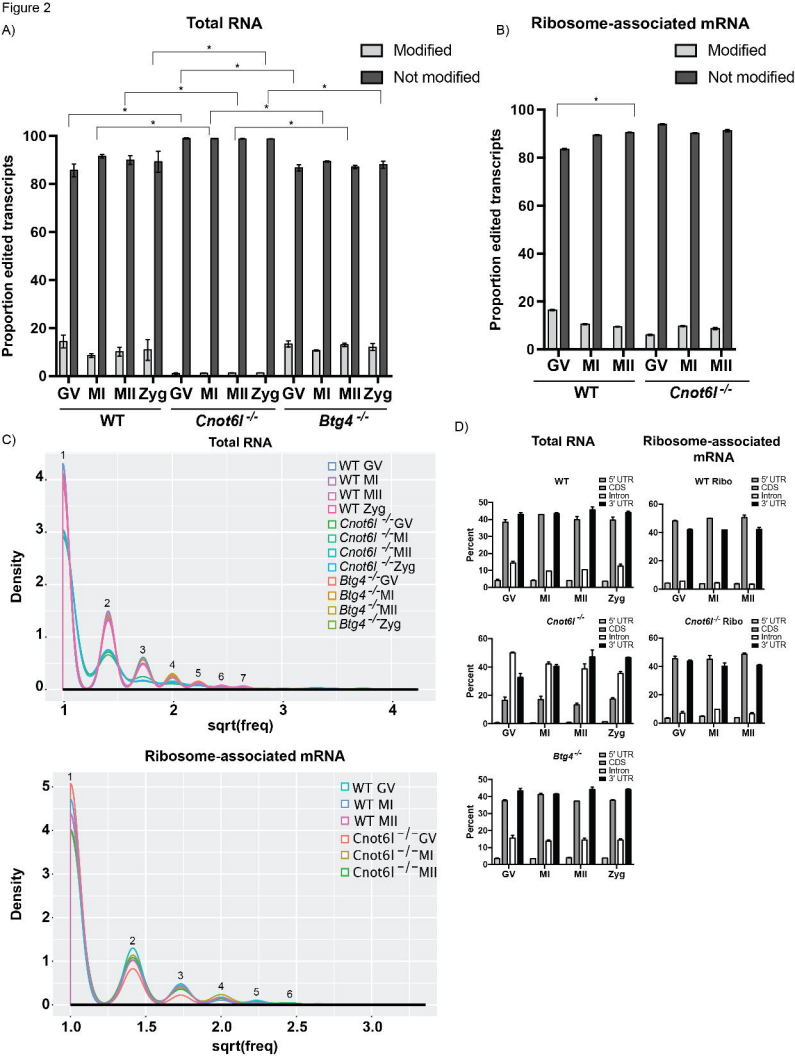
A)
Total RNA
Modified
Not modified
Proportion edited transcripts
GV MI MII Zyg GV MI MII Zyg GV MI MII Zyg
WT
Cnot6l -/-
Btg4 -/-
B)
Ribosome-associated mRNA
Modified
Not modified
Proportion edited transcripts
GV MI MII GV MI MII
WT
Cnot6l -/-
C)
Total RNA
WT GV
WT MI
WT MII
WT Zyg
Cnot6l -/-GV
Cnot6l -/-MI
Cnot6l -/-MII
Cnot6l -/-Zyg
Btg4 -/-GV
Btg4 -/-MI
Btg4 -/-MII
Btg4 -/-Zyg
Density
sqrt(freq)
Ribosome-associated mRNA
WT GV
WT MI
WT MII
Cnot6l -/-GV
Cnot6l -/-MI
Cnot6l -/-MII
Density
sqrt(freq)
D)
Total RNA
Ribosome-associated mRNA
WT
WT Ribo
Cnot6l -/-
Cnot6l -/- Ribo
Btg4 -/-
5' UTR
CDS
Intron
3' UTR
Percent
GV MI MII Zyg

Figure 3

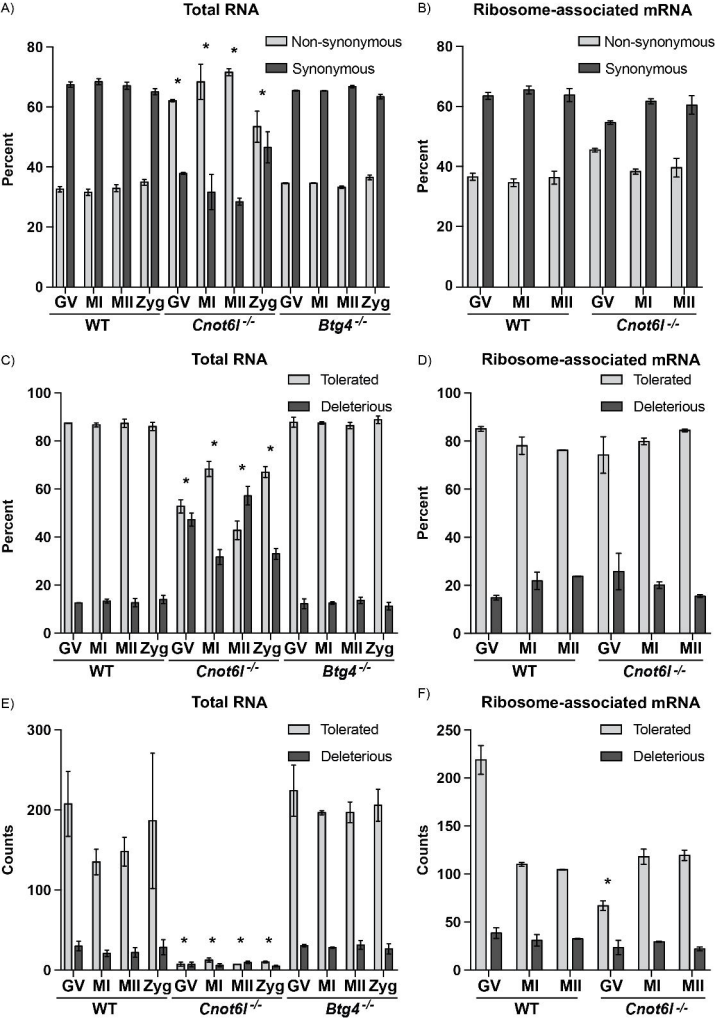
A)
Total RNA
Non-synonymous
Synonymous
Percent
GV MI MII Zyg GV MI MII Zyg GV MI MII Zyg
WT
Cnot6l -/-
Btg4 -/-
B)
Ribosome-associated mRNA
Non-synonymous
Synonymous
Percent
GV MI MII GV MI MII
WT
Cnot6l -/-
C)
Total RNA
Tolerated
Deleterious
Percent
GV MI MII Zyg GV MI MII Zyg GV MI MII Zyg
WT
Cnot6l -/-
Btg4 -/-
D)
Ribosome-associated mRNA
Tolerated
Deleterious
Percent
GV MI MII GV MI MII
WT
Cnot6l -/-
E)
Total RNA
Tolerated
Deleterious
Counts
GV MI MII Zyg GV MI MII Zyg GV MI MII Zyg
WT
Cnot6l -/-
Btg4 -/-
F)
Ribosome-associated mRNA
Tolerated
Deleterious
Counts
GV MI MII GV MI MII
WT
Cnot6l -/-

Figure 4

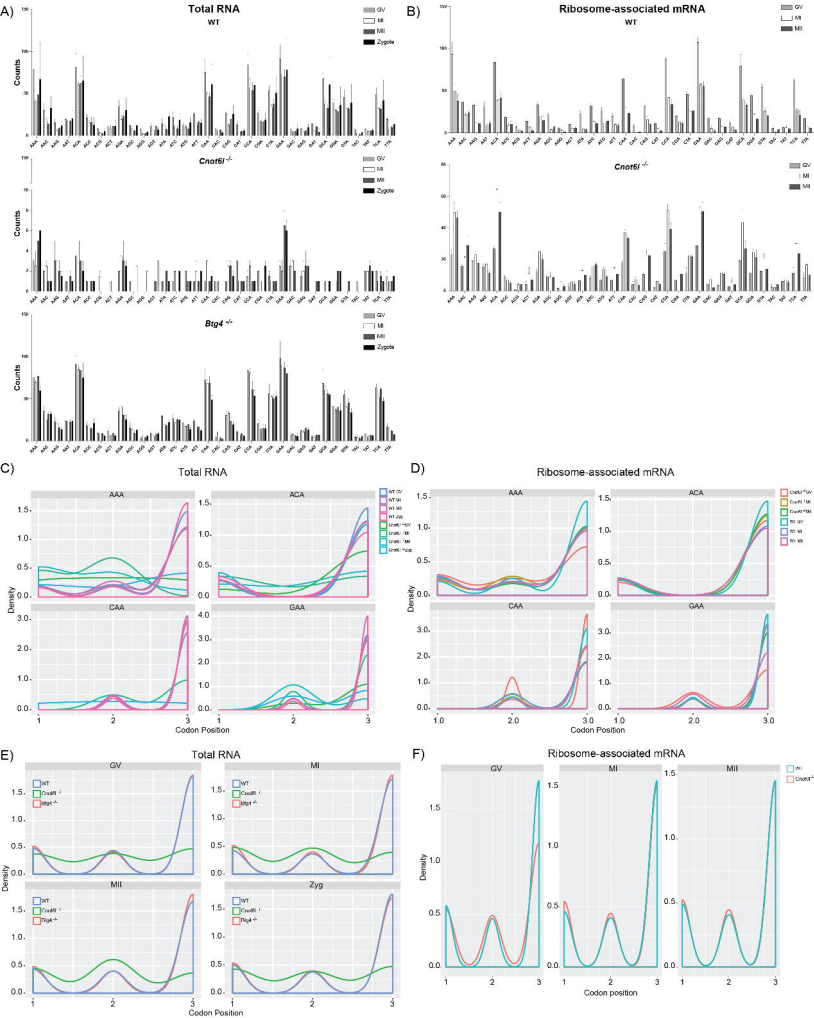
A)
Total RNA
WT
Cnot6l -/-
Btg4 -/-
Counts
GV
MI
MII
Zygote
B)
Ribosome-associated mRNA
WT
Cnot6l -/-
C)
Total RNA
AAA
ACA
CAA
GAA
Density
Codon Position
D)
Ribosome-associated mRNA
E)
Total RNA
GV
MI
MII
Zyg
WT
Cnot6l -/-
Btg4 -/-
F)
Ribosome-associated mRNA
Codon position

Figure 5

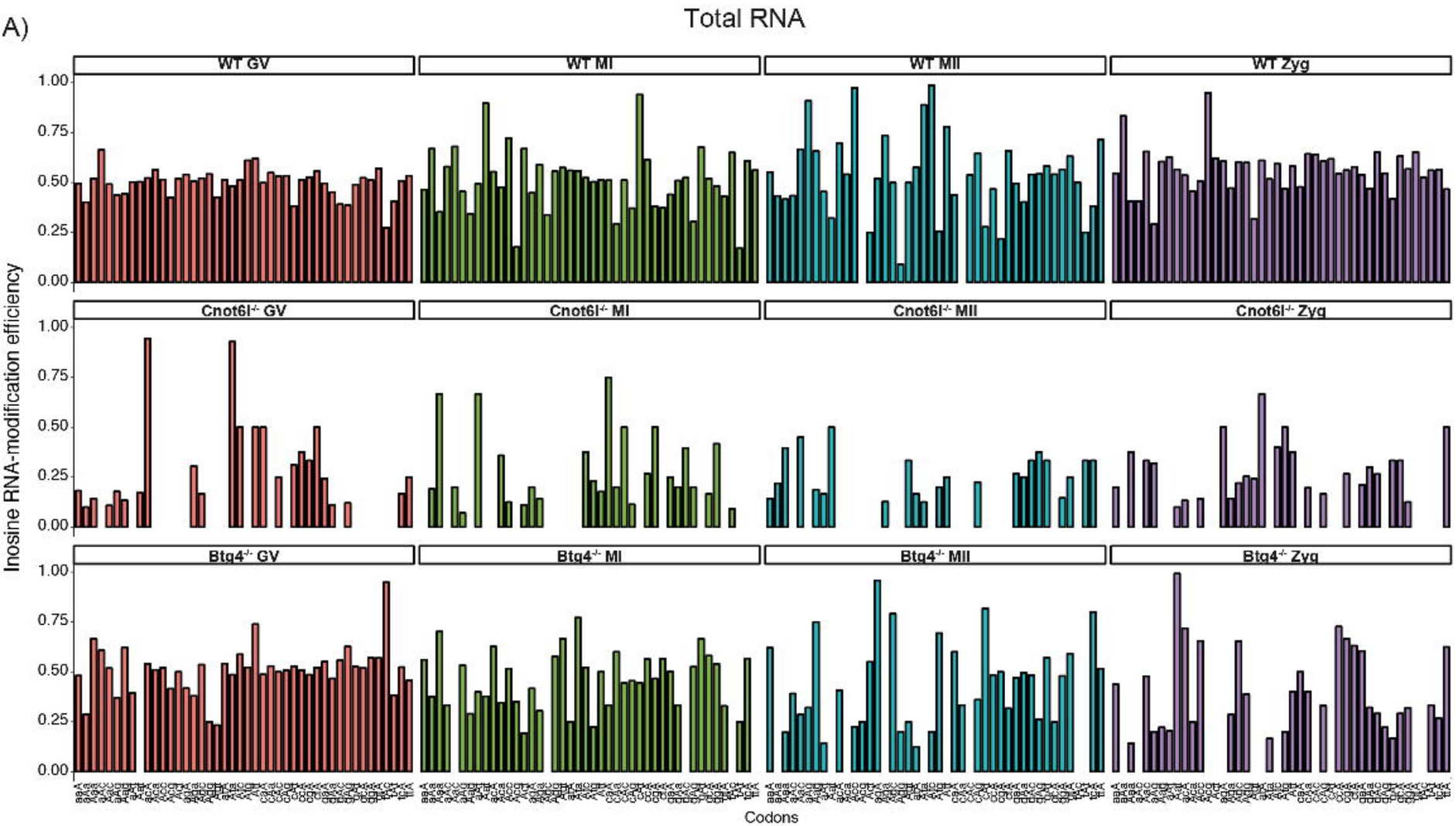
A)
Total RNA
WT GV
WT MI
WT MII
WT Zyg
Cnot6l-/- GV
Cnot6l-/- MI
Cnot6l-/- MII
Cnot6l-/- Zyg
Btg4-/- GV
Btg4-/- MI
Btg4-/- MII
Btg4-/- Zyg
Inosine RNA-modification efficiency
1.00
0.75
0.50
0.25
0.00
Codons

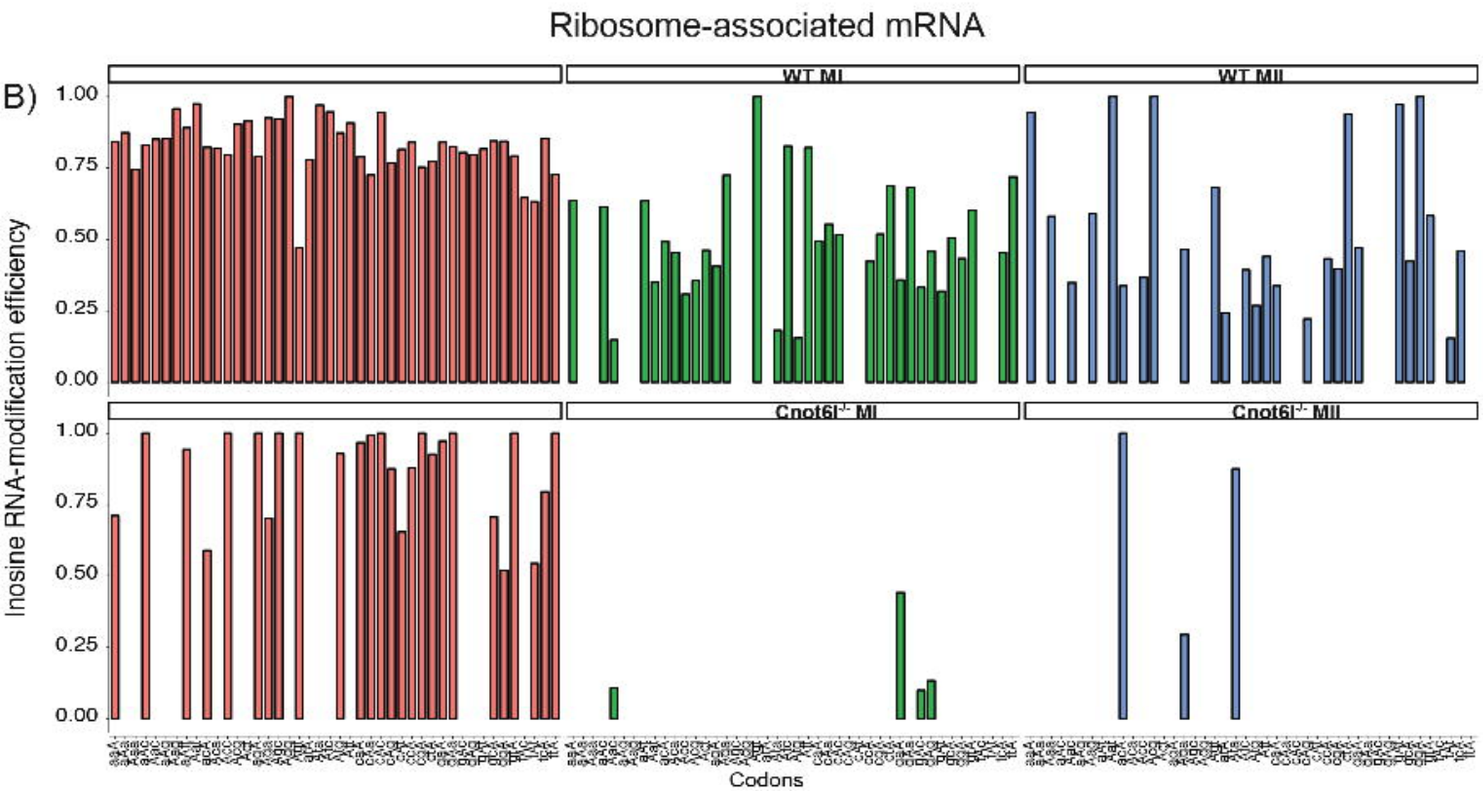
Ribosome-associated mRNA
B)
WT MI
WT MII
Cnot6l-/- MI
Cnot6l-/- MII
Inosine RNA-modification efficiency
1.00
0.75
0.50
0.25
0.00
Codons